

# Theory of excited state absorptions in phenylene-based $\pi$ -conjugated polymers

Alok Shukla,<sup>1</sup> Haranath Ghosh,<sup>2</sup> and Sumit Mazumdar<sup>3</sup>

<sup>1</sup>Physics Department, Indian Institute of Technology, Mumbai 400076, India

<sup>2</sup>Centre for Advanced Technology, Indore 452013, India

<sup>3</sup>Department of Physics, University of Arizona, Tucson, AZ 85721

(Dated: June 19, 2018)

Within a rigid-band correlated electron model for oligomers of poly-(paraphenylene) (PPP) and poly-(paraphenylenevinylene) (PPV), we show that there exist two fundamentally different classes of two-photon  $A_g$  states in these systems to which photoinduced absorption (PA) can occur. At relatively lower energies there occur  $A_g$  states which are superpositions of one electron - one hole (1e-1h) and two electron - two hole (2e-2h) excitations, that are both comprised of the highest delocalized valence band and the lowest delocalized conduction band states only. The dominant PA is to one specific member of this class of states (the  $mA_g$ ). In addition to the above class of  $A_g$  states, PA can also occur to a higher energy  $kA_g$  state whose 2e-2h component is *different* and has significant contributions from excitations involving both delocalized and localized bands. Our calculated scaled energies of the  $mA_g$  and the  $kA_g$  agree reasonably well to the experimentally observed low and high energy PAs in PPV. The calculated relative intensities of the two PAs are also in qualitative agreement with experiment. In the case of ladder-type PPP and its oligomers, we predict from our theoretical work a new intense PA at an energy considerably lower than the region where PA have been observed currently. Based on earlier work that showed that efficient charge-carrier generation occurs upon excitation to odd-parity states that involve both delocalized and localized bands, we speculate that it is the characteristic electronic nature of the  $kA_g$  that leads to charge generation subsequent to excitation to this state, as found experimentally.

PACS numbers: 78.47.+p, 78.20.Bh, 42.65.Re, 78.40.Me, 78.66.Qn

## I. INTRODUCTION

The applications of  $\pi$ -conjugated polymers in optical emission devices such as organic light emitting diodes<sup>1</sup> and laser active media<sup>2,3,4</sup> have led to intensive investigations of photoluminescent materials like PPP and PPV, their derivatives, and structurally related ladder type materials. Nonlinear spectroscopy, including both ultrafast photoinduced absorption (PA) measurements<sup>5,6,7,8,9,10,11,12,13,14</sup> and third order nonlinear optical measurements like electroabsorption (EA)<sup>7,15,16</sup>, third harmonic generation (THG)<sup>17</sup> and two-photon absorption (TPA)<sup>9,18,19</sup> have been carried out extensively to probe the even parity excited states that are dark under one-photon excitation but are two-photon allowed. In particular, interest in PA experiments stems from the observation that PA at high energies is followed by charge separation, with the creation of charged polarons on neighboring chains. Derivatives of PPV, for example, have been investigated by Frolov *et al.*<sup>8,9</sup>, who found two distinct PA bands in these systems, “low energy” PA1 and “high energy” PA2, occurring at  $\sim 0.8$  eV and  $\sim 1.3 - 1.4$  eV, respectively. Frolov *et al.* ascribe PA1 to the excited state absorption from the optical  $1B_u$  state to the so-called  $mA_g$  state (where  $m$  is a chain length dependent unknown quantum number), whose nature has been discussed extensively by theorists in the context of nonlinear spectroscopy of both luminescent polymers like PPV as well as nonluminescent linear chain polyacetylenes and polydiacetylenes<sup>20,21,22,23,24,25,26,27</sup>. PA2 has been ascribed by Frolov *et al.* to the excited state ab-

sorption to a higher energy  $kA_g$  state (where  $k$  is again an unknown quantum number), whose counterpart does not exist in the linear chain polymers, according to these authors. Interestingly, the relaxation dynamics of PA1 and PA2 are very different: while the  $mA_g$  decays back to the optical  $1B_u$  exciton by internal conversion, the  $kA_g$  undergoes a different relaxation pathway that leads to dissociation into long-lived polaron pairs that are probably interchain. Based on this, the authors have speculated that the electronic character of the  $kA_g$  is different from the  $mA_g$ .

Similar behavior have been observed by several different groups<sup>10,11,12,13,14</sup>, who have studied both PPV derivatives and structurally related materials like polyfluorene, ladder-type PPP and oligomers of the latter. There exist apparent subtleties in comparing some of these experimental results with those of Frolov *et al.*<sup>8,9</sup>, as the PA measurements in some of these cases were carried out only in the high energy region ( $> 1.4$  eV)<sup>13,14</sup>, and therefore the induced absorption termed PA1 by these latter authors actually corresponds to PA2 of Frolov *et al.*<sup>8,9</sup> (see section V for details). Apart from this difference in nomenclature, the fundamental observation in all cases appear to be the same, viz.,  $A_g$  states beyond some threshold energy mediate interchain charge-transfer. As an aside, we remark that it has also been claimed from ultrafast PA measurements in the wavelength region of infrared active vibrational modes that charge carriers are generated directly at the optical threshold, and that the quantum efficiency of charge generation is wavelength independent<sup>28,29</sup>. This last conclusion has, however, been challenged by Silva *et al.*<sup>12</sup>, whose demonstrations that

ultrafast photogeneration of charge carriers in a polyfluorene derivative is a consequence of sequential absorption to an  $A_g$  state that is at nearly twice the energy of the optical exciton (note that this is different from the  $kA_g$ ), and that there occur negligible yield of polarons under continuous wave conditions (where excitation to high energy  $A_g$  states does not occur) argue against the direct photogeneration scenario. The occurrence of EA<sup>15,30</sup> and TPA<sup>9</sup> at the same energy where PA2 occurs are yet other demonstrations of the existence of a  $kA_g$  state that is dipole-coupled to the  $1B_u$ . Recent photo-current excitation cross-correlation experiments<sup>31,32</sup> also support the sequential absorption picture. We shall therefore make no further comments on the experiments by Moses *et al.*<sup>28,29</sup>, which in any case is of secondary interest of this work; our primary interest is to understand the different electronic natures of the  $mA_g$  and the  $kA_g$  at a qualitative level.

Initial progress in theoretical understanding of possibly different classes of even parity states in phenylene-based conjugated polymers was made by Chakrabarti and Mazumdar<sup>33</sup>, who examined the excited states of biphenyl and triphenyl within the Pariser–Parr–Pople model<sup>34,35</sup>. Although many-body techniques used by these authors were accurate (exact and quadruple-CI, hereafter QCI), the basis sets used were limited and included only the degenerate pairs of highest occupied molecular orbitals (HOMOs) and lowest unoccupied molecular orbitals (LUMOs) of benzene. Each pair of degenerate MOs consists of a delocalized MO and a localized MO, with the  $\pi$  electron densities vanishing on the para carbon atoms in the latter<sup>36,37,38,39</sup>. Chakrabarti and Mazumdar showed that the two-photon states in these molecules were not only superpositions of 1e–1h and 2e–2h excitations involving the delocalized bonding ( $d$ ) and antibonding ( $d^*$ ) MOs, there occurred also strong admixing with 2e–2h excitations involving localized bonding ( $l$ ) and antibonding ( $l^*$ ) MOs. The authors therefore suggested that there occurred multiple kinds of  $A_g$  states in phenylene-based conjugated polymers. According to these authors,  $A_g$  states upto some threshold could qualitatively be understood within the space of  $d$  and  $d^*$  MOs only. The  $mA_g$  belongs to this class of  $A_g$  states. Beyond the threshold, however, there occurs a crossover to  $A_g$  states which have strong contributions from 2e–2h excitations involving  $l$  and  $l^*$  MOs. We shall hereafter write such states as  $(d \rightarrow l^*)^2$  and  $(l \rightarrow l^*)^2$  double excitations (as opposed to the  $(d \rightarrow d^*)^2$  double excitations with lower energies). Note that in all cases we do not make finer distinctions between configurations in which the hole or electron pairs occupy the same or different MOs (thus  $(d \rightarrow l^*)^2$  includes the 2e–2h excitations  $(d \rightarrow l^*; l \rightarrow d^*)$ ). According to these authors, the  $kA_g$  belonged to this second class of  $A_g$  states. No attempt was made to explain the charge separation and the calculations were limited strictly to explaining the possible difference between the  $mA_g$  and the  $kA_g$ .

The calculations by Chakrabarti and Mazumdar<sup>33</sup> are

suggestive but far from complete. Firstly, all calculated  $A_g$  states appeared to have nearly equal admixtures of  $(d \rightarrow d^*)^2$ ,  $(d \rightarrow l^*)^2$ ,  $(l \rightarrow d^*)^2$  and  $(l \rightarrow l^*)^2$ , which would appear to contradict the conjecture about different classes of  $A_g$  states. It was claimed that the strong mixing between different classes of 2e–2h excitations was a consequence of the severe length restrictions in the previous calculations and that with increasing conjugation length distinct  $A_g$  states dominated by different kinds of 2e–2h excitations would emerge. The actual demonstration of this requires going beyond the earlier small oligomer calculations. A second shortcoming of the earlier calculations is that they completely ignored the outer delocalized MOs of each benzene (as well as the MOs due to the vinylene segments in case of PPV). The complete band structure of PPV can be seen, for example, in reference 38, where one finds that in addition to the innermost delocalized valence and conduction bands (referred to as simply  $d$  and  $d^*$  in the above, but hereafter as  $d_1$  and  $d_1^*$ ) there occur also outer delocalized bands ( $d_2$  and  $d_2^*$ ;  $d_3$  and  $d_3^*$ ) that lie below (above) the  $l$  ( $l^*$ ) bands (the difference between PPV and PPP is the absence of the outermost  $d_3$  and  $d_3^*$  bands in PPP). The neglect of the outer  $d$ -bands raises the question whether higher energy PA is not to qualitatively different  $A_g$  states involving the localized levels, but to states that are dominated by excitations involving the outer  $d$ -bands. Finally, the previous calculations were not useful for even qualitative comparisons of relative energies and oscillator strengths of theoretical PA1 and PA2, again a consequence of the very severe length restriction.

In view of the above, we believe that a thorough and accurate theoretical investigation of the two-photon states of oligomers of PPP and PPV is in order. In the present paper, we present large scale correlated calculations employing the multireference singles and doubles configuration interaction (MRSDCI) method<sup>40,41</sup> on longer oligomers of PPP and PPV within a correlated electron Hamiltonian. Unlike the previous calculations<sup>33</sup>, higher energy MOs or bands are not ignored. We take considerable care that the results we report are accurate, by imposing strict convergence criteria on our MRSDCI calculations. For PPP, calculations are presented for oligomers containing three to five benzene rings. We refer to these as PPP3, PPP4 and PPP5, respectively. In the case of PPV, we consider oligomers that terminate with benzene molecules at both ends, in order to preserve spatial symmetry, and present MRSDCI results for oligomers containing three (PPV3) and four (PPV4) benzene rings. While these oligomers are still relatively short, we believe that it is far more important to incorporate electron correlation effects to high order than to go to longer oligomers.

The results of our calculations can be summarized as follows. Firstly, our computed PA spectra resemble the experimental PA spectra qualitatively: in all cases we find the theoretical PA1 to be much stronger than PA2. We discuss why the calculated  $A_g$  states are expected

to occur at energies where PA1 and PA2 are observed experimentally. Secondly, our present relatively longer chain calculations do indeed find lower and higher energy two-photon states whose 2e-2h components are significantly different, as would be required to claim that these belong to distinct classes. The different nature of the higher energy two-photon state that we believe to be the  $kA_g$  may explain the charge separation from this state. While this last statement is a speculation currently, it is supported by earlier photocurrent studies<sup>42</sup>. A third result involves our determination that the  $mA_g$  is not the lowest two-photon excited state in any of the systems we have studied (i.e., the quantum number  $m > 2$ ), even though the  $2A_g$  occurs above the  $1B_u$  in these systems. This particular result is in agreement with other recent theoretical work based on the limited basis of  $d_1$  and  $d_1^*$  bands<sup>43,44</sup>. As we remark later, this may also have experimental significance. Finally, we also find that as observed before from fittings of the linear absorption in PPV films<sup>45</sup>, the standard Ohno parameters<sup>46</sup> may be too large for even qualitative fittings of the PA at high energies, and a previously used phenomenological screened Coulomb parametrization<sup>45</sup> gives more satisfactory results.

In the next section we present our theoretical model and discuss the details of the MRSDCI approach as adopted here. In section III we present a brief review of the theory of linear absorption in the polyphenylenes, to point out that there occur distinct classes of one-excitation in the systems of interest, thereby suggesting the idea of distinct two-excitations. In section IV we present our theoretical results. This is followed by our conclusions and discussions of the scope of future work.

## II. THE THEORETICAL MODEL AND METHODOLOGY

We consider oligomers of PPP and PPV within the Pariser-Parr-Pople model Hamiltonian,

$$H = - \sum_{\langle ij \rangle, \sigma} t_{ij} (c_{i\sigma}^\dagger c_{j\sigma} + c_{j\sigma}^\dagger c_{i\sigma}) + U \sum_i n_{i\uparrow} n_{i\downarrow} + \sum_{i < j} V_{ij} (n_i - 1)(n_j - 1) \quad (1)$$

where  $\langle ij \rangle$  implies nearest neighbors,  $c_{i\sigma}^\dagger$  creates an electron of spin  $\sigma$  on the  $p_z$  orbital of carbon atom  $i$ ,  $n_{i\sigma} = c_{i\sigma}^\dagger c_{i\sigma}$  is the number of electrons with spin  $\sigma$ , and  $n_i = \sum_\sigma n_{i\sigma}$  is the total number of electrons on atom  $i$ . The parameters  $U$  and  $V_{ij}$  are the on-site and long-range Coulomb interactions, respectively, while  $t_{ij}$  is the nearest neighbor one-electron hopping matrix element that includes bond alternation and connectivity. The parametrization of the intersite Coulomb interactions is done in a manner similar to the Ohno parametrization<sup>46</sup>

$$V_{i,j} = U/\kappa(1 + 0.6117R_{i,j}^2)^{1/2}, \quad (2)$$

where  $\kappa$  is a parameter which has been introduced to account for the possible screening of the Coulomb interactions in the system<sup>45,47</sup>. We have examined both the standard Ohno parameters ( $U = 11.13$  eV,  $\kappa = 1.0$ ), as well as a particular combination of  $U$  and  $\kappa$  ( $U = 8.0$  eV,  $\kappa = 2.0$ ) that was shown previously to be satisfactory at a semiquantitative level for explaining the full wavelength dependent ground state absorption spectrum of PPV<sup>45</sup>. We shall hereafter refer to this second set of parameters as screened Ohno parameters. As far as the hopping matrix elements are concerned, we took  $t = -2.4$  eV for the C-C bond in benzene rings. The hopping corresponding to the interbenzene single bond in the PPP oligomers was taken to be  $t = -2.23$  eV. For the vinylene linkage of the PPV oligomers, we chose the hopping elements to be  $-2.2$  eV for the single bond, and  $-2.6$  eV for the double bond. We considered PPP and PPV oligomers in their planar configurations, with the conjugation direction along the  $x$  axis. Thus the symmetry group of PPP oligomers is  $D_{2h}$ , while that of PPV oligomers is  $C_{2h}$ . Since both symmetry groups have inversion as a symmetry element, the many electron states of these oligomers can be classified according to this symmetry. The two-photon states of both the PPP and PPV oligomers belong to the  $A_g$  irreducible representation (irrep) of the respective symmetry group, while the one-photon states belong to the  $B_u$  irrep for PPV, and  $B_{1u}$  ( $x$ -polarized), and  $B_{2u}$  ( $y$ -polarized) irreps for the oligo-PPPs. Since, here we are concerned mainly with the response of these systems to the  $x$ -polarized photons, therefore, henceforth, for PPP oligomers also we will refer to the  $B_{1u}$  states as  $B_u$  states. In all cases the calculated PA corresponds to the excited state absorption from the optical  $1B_u$  state. In all the many-body calculations presented in this work, full use of the stated point group symmetries was made.

As stated above, the correlated electron calculations were done using the MRSDCI approach, which is a powerful CI technique<sup>40</sup> that has been used previously for linear chain polyenes by Tavan and Schulten<sup>41</sup> as well as others<sup>25</sup>, and by us to calculate the excited state ordering in polyphenyl- and polydiphenylacetylenes<sup>48</sup>. As discussed in reference 48 we use very stringent convergence criterion for all excited states. The methodology behind the MRSDCI calculations is as follows. The calculations are initiated with a restricted Hartree-Fock (RHF) computation of the ground state of the oligomer concerned, followed by a transformation of the Hamiltonian from the site representation (Eq. 2) to the HF molecular-orbital representation. Subsequently, a singles-doubles CI (SDCI) calculation is performed, the different excited states in  $A_g$  and  $B_u$  subspaces are examined, and the  $N_{ref}$  configuration state functions (CSFs) making significant contributions to their many-particle wave functions are identified. The next step is the MRSDCI calculation for which the reference space consists of the  $N_{ref}$  CSFs identified in the previous step, and the overall Hamiltonian matrix now includes configurations that are singly and doubly excited with respect to these reference CSFs

(thereby including the dominant triply and quadruply excited configurations). The new ground and excited states are now re-examined to identify new CSFs contributing significantly to them so as to augment the reference space for the next set of MRSDCI calculations. This procedure is repeated until satisfactory convergences in the excitation energies of the relevant states are achieved. By the time convergence is achieved typically all CSFs with coefficients of magnitude 0.1 or more in the corresponding many-particle wave functions have been included in the MRSDCI reference space. Naturally, this leads to very large CI matrices. To give some idea of the highly correlated nature of the wavefunctions of the excited states we have examined and the level of accuracy in our calculations, in Table I we have listed the number of reference functions that were used for each symmetry subspace of PPP3, PPP4 and PPP5, respectively, as well as the overall sizes of the Hamiltonian matrix in each case (note that for PPP3 the method used was QCI rather than MRSDCI). The number of MRSDCI reference functions are larger in the  $A_g$  subspaces than in the  $B_u$  subspace because while only the  $1B_u$  was optimized in the  $B_u$  subspace, many different  $A_g$  states (all those with significant transition dipole couplings with the  $1B_u$ ) had to be simultaneously optimized in the  $A_g$  subspace. The  $N_{ref}$  in Table I should be compared to the few (usually 2 or 3) reference states that are retained in calculations of the lowest  $A_g$  states<sup>41</sup>. To the best of our knowledge, the present calculations are the most accurate correlated electron calculations that incorporate the full basis set for the polyphenylenes.

### III. THEORY OF GROUND STATE ABSORPTION AND ITS IMPLICATION

Before we present our calculations of PA, it is useful to recall the results of calculations of the ground state absorption<sup>36,37,38,39,45</sup>. This is because multiple classes of final states are relevant also in ground state absorption, and as we indicate below analysis of the ground state absorption strongly suggests that there should occur multiple classes of two-photon states. Within band theory ( $U = 0$ ) ground state absorption consists of 1e-1h excitations that are low energy  $d_1 \rightarrow d_1^*$ , high energy  $l \rightarrow l^*$ , and intermediate energy  $d_1 \rightarrow l^*$  and  $l \rightarrow d_1^*$ , with the intermediate energy absorption band occurring exactly half way in between the low and high energy absorption band. Here we have ignored absorptions involving  $d_2, d_2^*$  etc. bands, as excitations involving these bands lie outside the range of experimental wavelengths. The  $d_1 \rightarrow d_1^*$  and  $l \rightarrow l^*$  bands are polarized along the  $x$ -direction in PPP and predominantly along the  $x$ -direction in PPV, while the  $d_1 \rightarrow l^*$  and  $l \rightarrow d_1^*$  bands are polarized along the  $y$ -direction and predominantly along the  $y$ -direction, respectively. Experimentally in PPV there occur absorptions at  $\sim 2.4$  eV, 3.7 eV, 4.7 eV and  $\sim 6.0$  eV, respectively. These have been

explained within a correlated electron picture: absorptions at 2.4 eV and 6.0 eV are due to  $d_1 \rightarrow d_1^*$  and  $l \rightarrow l^*$  exciton states, respectively<sup>36,37,39,45</sup> the absorption at 3.7 eV is to a higher energy  $d_1 \rightarrow d_1^*$  exciton<sup>45</sup>; and finally, the absorption at 4.7 eV is to the “plus” linear combination of the excitations  $d_1 \rightarrow l^* + l \rightarrow d_1^*$ <sup>36,37,39,45</sup>. The corresponding “minus” linear combination,  $d_1 \rightarrow l^* - l \rightarrow d_1^*$ , occurs also at about 3.7 eV<sup>36,37,39,45</sup>, but is forbidden in linear absorption. All of these assignments have been confirmed by polarization studies of absorptions in stretch-oriented samples<sup>45,49,50</sup>.

The relevance of these known results to the present case are as follows. Energetically, the  $kA_g$  in PPV is at  $\sim 3.6 - 3.8$  eV<sup>8,9</sup>. Since ground state absorption occurs to a high energy  $d_1 \rightarrow d_1^*$  excitation of  $B_u$  symmetry in this energy region, in principle, the  $kA_g$  can simply be a similar  $d_1 \rightarrow d_1^*$  excitation of  $A_g$  symmetry. If this were true, the  $mA_g$  and the  $kA_g$  would be qualitatively similar, and charge carrier creation from the  $kA_g$  (but not from the  $mA_g$ ) can only be a consequence of possibly greater e-h separation in the  $kA_g$ . An alternate possibility is that the  $kA_g$  is dominated by configurations that are fundamentally different. Recall that the occurrence of the  $2A_g$  below the  $1B_u$  in polyacetylenes and polydiacetylenes is a general many-body phenomenon:  $A_g$  eigenstates having strong 2e-2h contributions from specific MOs can be close in energy, or can even occur below  $B_u$  eigenstates that are dominated by 1e-1h excitations involving the same MOs. Since the lowest energy 1e-1h excitations involving the  $d_1 \rightarrow l^*$  and  $l \rightarrow d_1^*$  excitations (the minus linear combinations mentioned above) occur at  $\sim 3.7$  eV, it is to be anticipated that many-body  $A_g$  eigenstates that are dominated by  $(d_1 \rightarrow l^*)^2$  and  $(l \rightarrow d_1^*)^2$  occur also within the same energy range. In principle then, the  $kA_g$  can also be dominated by 2e-2h components involving the  $l$  and  $l^*$  bands, and be qualitatively different from the  $mA_g$ . As shown in the following sections, we do indeed find evidence for such  $A_g$  states with significant dipole coupling to the  $1B_u$ .

### IV. RESULTS OF CORRELATED ELECTRON CALCULATIONS

#### A. Choice of parameters

As we show below electron correlation effects on different kinds of CSFs are different. This necessitates proper choice of the Coulomb parameters in Eq. 1. Here we show that the bare Ohno parameters are not suitable for high energy states of PPP and PPV. In Fig. 1 we show the calculated excited state absorption from the  $1B_u$  state for PPP3, for the case of Ohno parameters, obtained with the QCI approach. The spectral features I and II are due to the  $2A_g$  and the  $4A_g$  states of the oligomer, respectively, while the strong feature III has contributions from both the  $7A_g$  and the  $8A_g$ . The close proximity of spectral feature I to the  $1B_u$  in the theoretical spectrum

makes this outside the wavelength range within which the experimental PA features are observed. In principle, it might be possible to observe this  $2A_g$  state in TPA. In reality, Fig. 1 indicates that the strength of the TPA to the  $2A_g$  would be rather weak. This is because the calculated PA in Fig. 1 corresponds to linear absorption from the  $1B_u$  and hence consists of only positive terms; in contrast, the third order susceptibility corresponding to TPA contains both positive and negative terms<sup>51</sup>, and the relative strength of the  $2A_g$  peak in Fig. 1 therefore corresponds to an upper limit for TPA. Thus only calculated PA features II and III in Fig. 1 should be compared to experiments. The relative oscillator strengths of II and III are exactly opposite to the relative oscillator strengths of PA1 and PA2, which makes the calculated PA inconsistent with experiments<sup>8,9</sup>.

In order to probe this further, we have examined the final states of all PA features in considerable detail. Each of these wavefunctions is highly correlated, and is a superposition of numerous configurations. In order to obtain broad classifications of the different  $A_g$  states we expand the correlated wavefunction as,

$$|nA_g\rangle = \sum_i a_i |d_1 \rightarrow d_1^*\rangle_i + \sum_j b_j |(d_1 \rightarrow d_1^*)^2\rangle_j + \sum_k c_k |(d_1 \rightarrow l^*)^2\rangle_k + \dots \quad (3)$$

In the above  $nA_g$  is an arbitrary  $A_g$  state and each term on the right hand side contains all CSFs of a given class (for example,  $|d_1 \rightarrow d_1^*\rangle_i$  is the  $i$ th configuration of the type  $d_1 \rightarrow d_1$  whose coefficient in  $nA_g$  is  $a_i$ ). The right hand side of Eq. 3 is obviously not complete and the .... implies the existence of many other types of excitations  $d_1 \rightarrow d_2^*$ ,  $(d_1 \rightarrow d_2^*)^2$ , etc. Once terms have been collected in the above manner, it is possible to quantify the overall contribution of excitations of a given kind (for example,  $\sum_i |a_i|^2$  is the total contribution by excitations of the type  $d_1 \rightarrow d_1^*$ ). In Table II we have given the contributions of each kind of excitation that describe the  $2A_g$ ,  $4A_g$ ,  $7A_g$  and  $8A_g$  wavefunctions. The overall sum of the contributions corresponding to each  $A_g$  state does not add up to 1, since we have retained only the important excitations with coefficients at least 0.1 in our expansions of the wavefunctions. As seen from Table II, the  $2A_g$  wavefunction is very similar to the  $2A_g$  of linear chain polyenes, in that it is predominantly a superposition of 1e-1h  $d_1 \rightarrow d_1^*$  and 2e-2h  $(d_1 \rightarrow d_1^*)^2$  excitations. This supports the earlier application of the effective linear chain model for the description of this state in PPV and PPP<sup>52</sup>. The two states  $7A_g$  and  $8A_g$  also have strong contributions from  $(d_1 \rightarrow d_1^*)^2$ , and weak contributions from  $(d_1 \rightarrow l^*)^2$  or  $(l \rightarrow d_1^*)^2$ . These states are therefore physically related to the  $mA_g$  that has been discussed before in the context of nonlinear spectroscopy. In contrast to the above states, the  $4A_g$  has much stronger contribution from  $(d_1 \rightarrow l^*)^2$  and  $(l \rightarrow d_1^*)^2$ . The occurrence of a

$(d_1 \rightarrow l^*)^2$  and  $(l \rightarrow d_1^*)^2$  type state *below* the predominantly  $(d_1 \rightarrow d_1^*)^2$  states suggests that (a) electron correlation effects are stronger on CSFs involving the localized MOs than on CSFs involving only delocalized MOs, and (b) the bare Ohno Coulomb parameters are too strong to describe PPP or PPV films, since it is the large magnitude of the Ohno correlation parameters that causes the effective crossing of eigenfunctions of different types, which in turn leads to the reversal of the intensities of the absorption bands as a function of energy.

Although in the above we have shown the theoretical PA spectrum only for PPP3, we emphasize that identical behavior is seen with the Ohno parameters for PPP4, PPP5, PPV3 and PPV4. In all cases the intensity profile of the excited state absorption is opposite to that observed experimentally, and wavefunction analysis indicates that this is due to the ordering of the states as in the above.

That the Ohno parameters are too large for high energy states of PPV, PPP etc. was suggested earlier from calculations of ground state absorption of PPV<sup>53</sup>. With the Ohno parameters, the calculated  $l \rightarrow l^*$  absorption (polarized along the  $x$ -direction) occurs below the calculated  $(d_1 \rightarrow l^* + l \rightarrow d_1^*)$  absorption ( $y$ -polarized)<sup>53</sup>, in contradiction to polarized absorption experiments<sup>45,49,50</sup>. As pointed out in reference 53, this last theoretical result was obtained even for trans-stilbene in one of the earliest computational works<sup>54</sup>. Very recently, Castleton and Barford<sup>47</sup> have done careful analysis of a very large number of high energy excited states in benzene, biphenyl and trans-stilbene using full-CI and have reached the same conclusion. Within Eq. 2, the authors suggest  $U = 7.2$  eV and  $\kappa = 1.36$  for the hydrocarbon matrix condensed phases of the above molecules, along with finer modifications of the hopping integrals. These values of  $U$  and  $\kappa$  are close to the  $U = 8$  eV and  $\kappa = 2.0$  that were suggested in reference<sup>53</sup>, and that we use in our calculations in the next section. Given that our goal is semiquantitative only (recall that our calculations are for relatively short oligomers while the available experimental results include those for much longer chains) finetuning of the parameters as done by Castleton and Barford would be premature. The necessity to incorporate screening of the bare Ohno Coulomb parameters in order to fit the high energy excited states in condensed phases of conjugated polymers have also been discussed by Moore and Yaron<sup>55</sup>, from a different perspective.

## B. PA spectra with screened Coulomb parameters

In Fig. 2 we have shown the calculated excited state absorptions for (a) PPP4, (b) PPP5, (c) PPV3 and (d) PPV4 for  $U = 8.0$  eV and  $\kappa = 2$ . In all cases our abscissa is the energy scaled with respect to  $E(1B_u)$ . As pointed out before<sup>56</sup>, convergence in the scaled energies of high energy states with increasing chain length is not expected in this region of relatively short chain lengths. This is be-

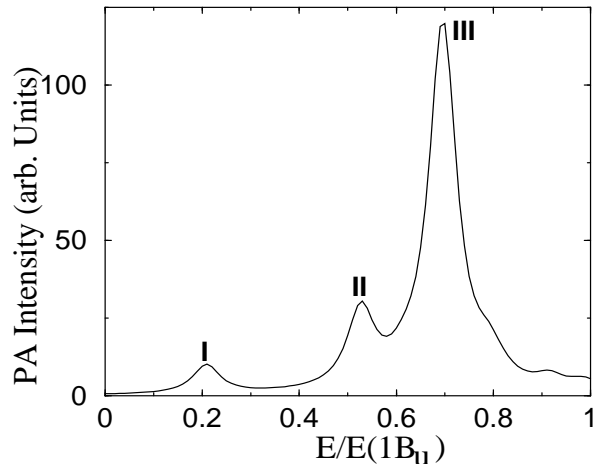


FIG. 1: Calculated PA spectrum of PPP3, with the standard Ohno Coulomb parameters. A linewidth of 0.15 eV was assumed.

cause the lowest energy excitations (for example, the  $1B_u$  and the  $2A_g$ ) converge with increasing chain length much faster than the higher energy states. Taken together with the discrete nature of the excited states, this can indicate an *apparent* increase in the scaled energy of the high energy excited state with increasing chain length, even as the actual energy is decreasing. This is exactly what happens between PPP4 and PPP5, and between PPV3 and PPV4 in Fig. 2. Quantitative comparisons of the scaled energies of the theoretical excited state absorption bands and those of the experimental PA bands thus cannot be expected, particularly in view of the fact that the relative location of the  $A_g$  state dominated by  $(d_1 \rightarrow l^*)^2$  excitations is very sensitive to relatively minor changes in the Coulomb correlation parameters (see previous subsection and also below). The energies and the relative intensities of the theoretical induced absorptions are therefore for semiquantitative comparisons only. From Figs. 2(c) and 2(d), it can be concluded that PA1 in PPV derivatives is due to the calculated spectral feature II which peaks slightly below  $0.4 \times E(1B_u)$ , which would correspond to about 0.9 eV in long chain PPV derivatives (with  $E(1B_u) \sim 2.2$  eV). This is quite close to experimental PA1 energy in PPV derivatives<sup>8,9</sup>. We remark on the PA energies in PPP derivatives in the next section, where more detailed comparisons to experiments are made. In all cases, the theoretical PA feature I corresponds to the  $2A_g$  (see below), and the close proximity of this state to the  $1B_u$  again suggests that this state is outside the wavelength region within which experimental PA has been observed.

For detailed understanding, in Table III we have described the wavefunctions of each of the final  $A_g$  states corresponding to each band in the calculated PA spectra. The items in Table III are similar to those in Table II, i.e., each entry corresponds to the overall contribution

TABLE I: The number of reference configurations ( $N_{ref}$ ) and the total number of configurations ( $N_{total}$ ) involved in the MRSDCI (or QCI, where indicated) calculations, for different symmetry subspaces of the various oligomers.

Oligomer	$A_g$		$B_u$	
	$N_{ref}$	$N_{total}$	$N_{ref}$	$N_{total}$
PPP3	1 <sup>a</sup>	193678	1 <sup>a</sup>	335545
PPP4	55	284988	15	76795
PPP5	48	663619	7	87146
PPV3	37	215898	12	220905
PPV4	39	981355	3	225970

<sup>a</sup> QCI method

TABLE II: Relative weights of the dominant contributions to the excited states of PPP3, computed with the standard Ohno parameters (see text).

PA Feature	State	$d_1 \rightarrow d_1^*$	$d_1 \rightarrow d_2^*$	$(d_1 \rightarrow d_1^*)^2$	$(d_1 \rightarrow l^*)^2$
I	$2A_g$	0.3585	0.0601	0.2670	—
II	$4A_g$	0.0452	0.1521	0.1266	0.2282
III	$7A_g$	0.1116	0.1280	0.1152	0.0660
	$8A_g$	0.0939	0.0772	0.3155	0.0985

of each kind of an excitation. Remarkably, the wavefunction descriptions of the different spectral features are very similar for all four systems shown in Fig. 2. Broadly speaking, there occur three distinct classes of  $A_g$  states in all four systems. These are discussed below.

The first class of states is represented by the  $2A_g$ , which in all cases is predominantly a superposition of  $1e-1h$   $d_1 \rightarrow d_1^*$  and  $2e-2h$   $(d_1 \rightarrow d_1^*)^2$ , as with the Ohno parameters. However, compared to the bare Ohno parameters, the relative weight of the  $1e-1h$  excitations here is larger. This is a consequence of the smaller  $U$ , and is to be expected. Furthermore, the relative weight of the  $1e-1h$  excitations is also larger in the PPP oligomers than in the PPV oligomers. This is also to be expected, based on the larger one-electron gap in PPP. The  $2A_g$  can certainly be described within an effective linear chain model with large dimerization that retains only the  $d_1$  and  $d_1^*$  bands, as suggested before<sup>52</sup>.

The second class of states are represented in all cases by the different  $A_g$  states that form the final states in the second and third bands in the calculated PA spectra. These have strong contributions from  $2e-2h$   $(d_1 \rightarrow d_1^*)^2$ , and weak but nonzero contributions from  $(d_1 \rightarrow l^*)^2$  and  $(l \rightarrow d_1^*)^2$ . In addition, there occur also  $1e-1h$  contributions of the type  $d_1 \rightarrow d_2^*$ ,  $d_2 \rightarrow d_1^*$ , etc., and while there are subtle differences in the relative contributions by different kinds of single excitations involving low and high energy delocalized bands, the overall natures of the excitations that are the final states in absorption bands II and III are similar. The qualitative natures of these eigenstates are very similar to that of the  $mA_g$  discussed in the context of nonlinear spectroscopy of

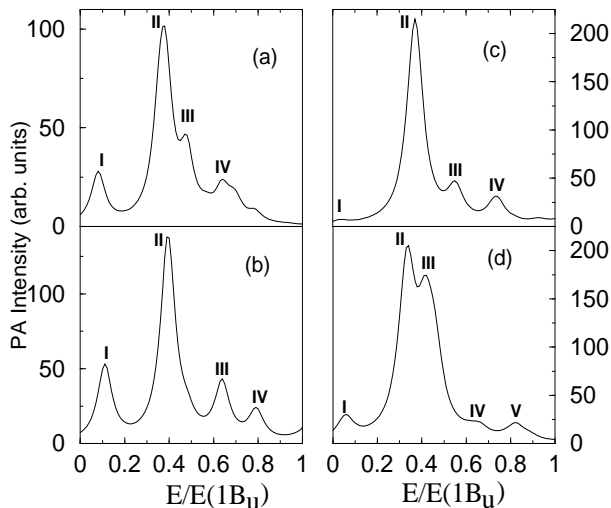


FIG. 2: Calculated PA spectra of (a) PPP4, (b) PPP5, (c) PPV3, and (d) PPV4, with screened Coulomb parameters. The scales for the intensity are different in different cases. A line width of 0.15 eV was assumed in all cases.

polyacetylenes and polydiacetylenes. The wavefunction descriptions make it clear that very qualitatively these wavefunctions can also be described within the effective linear chain model, but with less precision than the  $2A_g$ . Our calculated relative intensities of the  $2A_g$  and the  $mA_g$  are in qualitative agreement with other recent calculations for polyphenylenes that used a basis space of only the  $d_1$  and  $d_1^*$  bands<sup>43,44</sup>.

Above band III in the calculated spectra we always have a state that is qualitatively different from lower energy  $A_g$  states. This corresponds to the spectral feature IV in PPP4, PPP5 and PPV3, and the spectral feature V in PPV4. The relative weights of the two classes of 2e–2h excitations,  $(d_1 \rightarrow d_1^*)^2$  and  $(d_1 \rightarrow l^*)^2$ , are reversed in this high energy state, with the former now making weak contribution and the latter a strong contribution. This qualitative difference between the  $A_g$  states at different energies is in agreement with the earlier conjecture by Chakrabarti and Mazumdar<sup>33</sup>. The clear demarcation between  $A_g$  states dominated by either  $(d_1 \rightarrow d_1^*)^2$  or  $(d_1 \rightarrow l^*)^2$ , rather than nearly equal admixing, is a new result. This is an effect of increased oligomer length, as discussed above. Furthermore, we also notice that the highest energy two-photon states in Fig. 2 have the strongest 1e–1h contribution from excitations of the type  $d_1 \rightarrow d_2^*$  (in the case of PPP oligomers) and  $d_1 \rightarrow d_3^*$  (in the case of PPV oligomers). This is yet another difference between the  $mA_g$  and the  $kA_g$ . What is also significant is the weak role of  $(l \rightarrow l^*)^2$  2e–2h excitations in the  $A_g$  states included in Table III, in contrast to their relatively strong role in the high energy  $A_g$  states of biphenyl and triphenyl within the previous limited basis calculations<sup>33</sup>. This is also an effect of increased chain length, with the  $(l \rightarrow l^*)^2$  2e–2h excitations now perhaps dominating even

higher energy distinct two-photon states. The weaker oscillator strength of absorption band IV, relative to the strong oscillator strength of absorption band II is easily understood from Table III: 2e–2h excitations of the type  $(d_1 \rightarrow l^*)^2$  have small dipole coupling with the  $1B_u$ , which is predominantly  $d_1 \rightarrow d_1^*$ . Thus the dipole coupling of the  $A_g$  states responsible for absorption band IV originates mostly from the small 1e–1h contribution to this state. These highest energy  $A_g$  states are neither expected nor found in the limited basis calculations by Lavrentiev *et al.*<sup>43</sup> and Beljonne<sup>44</sup>.

Taken together, the results of Table III indicate the occurrence of different classes of  $A_g$  states, which are distinguished by the dominance of different types of 2e–2h excitations. With hindsight, this is perhaps not entirely surprising, as discussed in section III.

## V. CONCLUSIONS AND DISCUSSIONS

Even as the concept of different types of two-photon states appear to be correct, it might seem that straightforward assignments of experimental PA1 and PA2 from the calculated PA spectra of Fig. 2 alone are not possible. We first discuss applications of our theory to PPV derivatives, and then to ladder PPP, etc. The strong spectral feature II in the theoretical spectra (the theoretical  $mA_g$ ) is certainly a component of the experimental PA1 in PPV derivatives. Beyond this there are two possibilities, viz., (i) the spectral feature III corresponds to PA2, and the spectral feature IV (V in PPV4) is too high in energy to be observed experimentally; or (ii) the spectral feature III is also a part of PA1 (especially in long chains) and it is the high energy  $(d_1 \rightarrow l^*)^2$  excitation that corresponds to PA2. We ascribe the  $(d_1 \rightarrow l^*)^2$  excitation to PA2 based on the following reasons. First,  $A_g$  states that give rise to spectral feature III occur also in linear chain polyenes<sup>21</sup>. Their contribution to EA and TPA are vanishingly weak in long chains. In contrast, the contributions of the experimental  $kA_g$  to EA and TPA in PPV derivatives are clearly visible<sup>9,15,30</sup>. On the other hand, eigenstates that are predominantly  $(d_1 \rightarrow l^*)^2$  are clearly absent in polyacetylenes and polydiacetylenes, which possess only delocalized valence and conduction bands, and hence our assignment would naturally explain the absence of the  $kA_g$  state in these systems<sup>15,30</sup>. Second, as we have already remarked, spectral feature III (but not IV) has also been found in the calculations by Beljonne<sup>44</sup>, who, however, determined that in the long chain limit the energies of features II and III converge. This once again supports our assignment of the  $(d_1 \rightarrow l^*)^2$  excitation to PA2 (note also that the 1e–1h contributions of the highest energy two-photon states are different, further justifying the notion that these states belong to a different class from the lower energy  $2A_g$  and the  $mA_g$ ). We have already pointed out that the calculated PA1 energy is reasonably close to the experimental PA1 energy in PPV derivatives. The calculated scaled energy of PA2 from Figs. 2(c) and (d),

at  $0.7 - 0.8 \times E(1B_u)$  (again with experimental  $E(1B_u) = 2.2$  eV in substituted PPV's) is at  $1.5 - 1.76$  eV, which is a reasonably good fit to the experimental PA2 energy of  $1.3 - 1.4$  eV, given the very short lengths of our oligomers, and the increased difficulty of fitting of very high energy states.

As mentioned in section I, we believe that the recent experiments on a methyl-substituted ladder type PPP (*m*-LPPP)<sup>13</sup> and on a ladder type oligophenyl<sup>14</sup> have probed an energy region that is considerably above the region where the  $mA_g$  occurs. The PA features that have been called PA1 in these works occur at  $1.5$  eV in the polymer and at  $1.8$  eV in the oligomer, and are therefore too high in energy to be the same as PA1 in PPV derivatives. We therefore believe that the observed lowest energy PA features actually correspond to PA2 of Frolov *et al.*, and this is why charge separation occurs upon excitation to this energy. This assignment is supported by the observation of EA<sup>57</sup> as well as TPA<sup>58</sup> to a different lower energy two-photon state that occurs  $\sim 0.7$  eV above the  $1B_u$  exciton in the polymer. We therefore make the testable prediction that there should occur in these systems a lower energy PA at  $\sim 0.7$  eV that is considerably stronger than the PAs in the  $1.5 - 1.8$  eV range. The scaled PA2 energy from our PPP oligomer calculations,  $0.6 - 0.8 \times E(1B_u)$ , with experimental  $E(1B_u) = 2.7$  eV in *m*-LPPP<sup>57</sup>, corresponds to  $1.6 - 2.1$  eV, once again reasonably close to the experimental value.

The above then leads to the question why dissociation of the  $kA_g$  to polaron pairs is so efficient. We speculate that this is related to the specific structure of the  $kA_g$ . In photoconductivity measurement on a PPV derivative it has been found that a large jump in the photoconductivity occurs at  $4.7$  eV, exactly where the  $d_1 \rightarrow l^* + l \rightarrow d_1^*$  one-photon exciton is located<sup>42</sup>. The jump in the photoconductivity is due to a sudden increase in the interchain charge carrier generation subsequent to the excitation to this particular excited state. We speculate that there occurs a similar enhanced charge carrier generation subsequent to the sequential excitation to an  $A_g$  state that has strong contributions from  $(d \rightarrow l^*)^2$  (whose energy is however lower and close to the minus combination of the one-excitations). Indeed, similar mechanism has also been suggested by Zenz *et al.*<sup>31</sup>. In the original work by Köhler *et al.*, theoretical calculations suggested that the enhanced dissociation of the  $d_1 \rightarrow l^* + l \rightarrow d_1^*$  state was a

consequence of the highly delocalized electron-hole character of this state<sup>42</sup>. The latter necessarily implies that the charge carriers are similarly weakly bound even in the  $(d_1 \rightarrow l^*)^2$  double excitation. Additional contribution to the enhanced tendency to charge separation in the case of PPVs from excitations involving  $l$  and  $l^*$  bands may also come from phenyl ring rotations that occur in these excited states. Given that the charge densities on the para carbons are exactly zero for the  $l$  and  $l^*$  MOs, bond orders involving the para carbon atoms in the  $kA_g$  will be particularly small. This might lead to greater phenyl ring rotation in the  $kA_g$  than in the  $1B_u$  excitation. This feature of the  $kA_g$  can lead to a lifetime that is longer than the  $mA_g$ , and it is conceivable that the relatively long lifetime and the weak binding between the electrons and holes together contribute to the charge separation. In a recent work, one of us (S.M.) and colleagues have calculated the relative yields of singlet and triplet excitons starting from oppositely charged polarons, in the presence of interchain hopping of electrons and holes<sup>59,60</sup>. The computational technique used to calculate charge recombination in these works can be applied also to the opposite process of photoinduced charge transfer. Photoinduced charge transfer from different classes of  $A_g$  states is of interest in the present context and is currently being investigated.

Our observation that the  $2A_g$  is not the  $mA_g$  may also have experimental significance. An early measurement detected strong two-photon fluorescence in PPV from a state that is only  $0.5$  eV above the  $1B_u$ <sup>18</sup>, and evidence for a second two-photon state slightly higher in energy. Later experiments involving nonlinear absorption have invariably found the  $mA_g$  to be at least  $0.8$  eV above the  $1B_u$ . It is conceivable that the low energy two-photon state found by Baker *et al.* is the  $2A_g$ . A similar suggestion has also been made by Lavrentiev *et al.*<sup>43</sup>.

## VI. ACKNOWLEDGEMENTS

Work at Arizona was partially supported by NSF DMR-0101659, NSF ECS-0108696, and the ONR. We acknowledge many useful discussions with G. Lanzani and Z.V. Vardeny.

<sup>1</sup> R. H. Friend, R. W. Gymer, A. B. Holmes, J. H. Burroughes, R. N. Marks, C. Taliani, D. D. C. Bradley, D. A. D. Santos, J. L. Brédas, M. Logdlund, et al., *Nature* **397**, 121 (1999).

<sup>2</sup> N. Tessler, G. J. Denton, and R. H. Friend, *Nature* **382**, 695 (1996).

<sup>3</sup> F. Hide, M. A. Diaz-Garcia, B. J. Schwartz, M. R. Andersson, Q. Pei, and A. Heeger, *Science* **273**, 1833 (1996).

<sup>4</sup> S. V. Frolov, W. Gellermann, M. Ozaki, K. Yoshino, and

Z. V. Vardeny, *Phys. Rev. Lett.* **78**, 729 (1997).

<sup>5</sup> M. Yan, L. J. Rothberg, F. Papadimitrakopoulos, M. E. Galvin, and T. M. Miller, *Phys. Rev. Lett.* **72**, 1104 (1994).

<sup>6</sup> J. Hsu, M. Yan, T. M. Jedju, L. J. Rothberg, and B. R. Hsieh, *Phys. Rev. B* **49**, 712 (1994).

<sup>7</sup> J. Leng, S. Jeglinski, X. Wei, R. E. Benner, Z. V. Vardeny, F. Guo, and S. Mazumdar, *Phys. Rev. Lett.* **72**, 156 (1994).

<sup>8</sup> S. V. Frolov, Z. Bao, M. Wohlgenannt, and Z. V. Vardeny, *Phys. Rev. Lett.* **85**, 2196 (2000).



- <sup>9</sup> S. V. Frolov, Z. Bao, M. Wohlgenannt, and Z. V. Vardeny, *Phys. Rev. B* **65**, 205209 (2001).
- <sup>10</sup> V. I. Klimov, D. W. McBranch, N. Barashkov, and J. Ferraris, *Phys. Rev. B* **58**, 7654 (1998).
- <sup>11</sup> B. Kraabel, V. I. Klimov, R. Kohlman, S. Xu, H. L. Wang, and D. W. McBranch, *Phys. Rev. B* **61**, 8501 (2000).
- <sup>12</sup> C. Silva, A. S. Dhoot, D. M. Russell, M. A. Stevens, A. C. Arias, J. D. MacKenzie, N. D. Greenham, and R. H. Friend, *Phys. Rev. B* **64**, 125211 (2001).
- <sup>13</sup> C. Gadermaier, G. Cerullo, G. Sansone, G. Leising, U. Scherf, and G. Lanzani, *Phys. Rev. Lett.* **89**, 117402 (2002).
- <sup>14</sup> C. Gadermaier, G. Cerullo, M. Zavelani-Rossi, G. Sansone, G. Lanzani, E. Zojer, A. Pogantsch, D. Beljonne, Z. Shuai, J. L. Brédas, et al., *Phys. Rev. B* **66**, 125203 (2002).
- <sup>15</sup> M. Liess, S. Jeglinsky, Z. V. Vardeny, M. Ozaki, K. Yoshino, Y. Ding, and T. Barton, *Phys. Rev. B* **56**, 15712 (1997).
- <sup>16</sup> S. J. Martin, D. D. C. Bradley, P. A. Lane, H. Mellor, and P. L. Burn, *Phys. Rev. B* **59**, 15133 (1999).
- <sup>17</sup> A. Mathy, K. Ueberhofen, R. Schenk, H. Gregorius, R. Garay, K. Müllen, and C. Bubeck, *Phys. Rev. B* **53**, 4367 (1996).
- <sup>18</sup> C. J. Baker, O. M. Gelsen, and D. D. C. Bradley, *Chem. Phys. Lett.* **201**, 127 (1993).
- <sup>19</sup> U. Lemmer, R. Fischer, J. Feldmann, R. F. Mahrt, J. Yang, A. Greiner, H. Bässler, E. Göbel, H. Heesel, and H. Kurz, *Chem. Phys. Lett.* **203**, 28 (1993).
- <sup>20</sup> S. N. Dixit, D. Guo, and S. Mazumdar, *Phys. Rev. B* **43**, 6781 (1991).
- <sup>21</sup> M. Chandross, Y. Shimoi, and S. Mazumdar, *Phys. Rev. B* **59**, 4822 (1999).
- <sup>22</sup> P. C. M. McWilliams, G. W. Hayden, and Z. G. Soos, *Phys. Rev. B* **43**, 9777 (1991).
- <sup>23</sup> Z. G. Soos and R. G. Kepler, *Phys. Rev. B* **43**, 11908 (1991).
- <sup>24</sup> S. Abe, M. Schreiber, W. P. Su, and J. Yu, *Phys. Rev. B* **45**, 9432 (1992).
- <sup>25</sup> D. Beljonne, R. Cornil, Z. Shuai, J. Brédas, F. Rohlfiing, D. D. C. Bradley, W. E. Torruellas, V. Ricci, and G. I. Stegeman, *Phys. Rev. B* **55**, 1505 (1997).
- <sup>26</sup> D. Yaron, *Phys. Rev. B* **54**, 4609 (1996).
- <sup>27</sup> A. Race, W. Barford, and R. J. Bursill, *Phys. Rev. B* **64**, 035208 (2001).
- <sup>28</sup> D. Moses, A. Dogariu, and A. J. Heeger, *Phys. Rev. B* **61**, 9373 (2000).
- <sup>29</sup> P. B. Miranda, D. Moses, and A. J. Heeger, *Phys. Rev. B* **64**, 081201 (2001).
- <sup>30</sup> R. Österbacka, M. Wohlgenannt, M. Shkunov, D. Chinn, and Z. V. Vardeny, *J. Chem. Phys.* **xxx**, xxxx (2002).
- <sup>31</sup> C. Zenz, G. Lanzani, G. Cerullo, W. Graupner, G. Leising, U. Scherf, and S. DeSilvestri, *Synth. Metals* **116**, 27 (2001).
- <sup>32</sup> J. G. Müller, U. Scherf, and U. Lemmer, *Synth. Metals* **119**, 395 (2001).
- <sup>33</sup> A. Chakrabarti and S. Mazumdar, *Phys. Rev. B* **59**, 4839 (1999).
- <sup>34</sup> R. Pariser and R. G. Parr, *J. Chem. Phys.* **21**, 466 (1953).
- <sup>35</sup> J. A. Pople, *Trans. Faraday Soc.* **68**, 81 (1954).
- <sup>36</sup> M. J. Rice and Y. N. Gartstein, *Phys. Rev. Lett.* **73**, 2504 (1994).
- <sup>37</sup> J. Cornil, D. Beljonne, R. H. Friend, and J. L. Brédas, *Chem. Phys. Lett.* **223**, 82 (1994).
- <sup>38</sup> M. Chandross, S. Mazumdar, S. Jeglinski, X. Wei, Z. V. Vardeny, E. W. Kwock, and T. M. Miller, *Phys. Rev. B* **50**, 14702 (1994).
- <sup>39</sup> Y. Shimoi and S. Abe, *Synth. Metals* **78**, 219 (1996).
- <sup>40</sup> R. J. Buenker and S. D. Peyerimhoff, *Theor. Chim. Acta* **35**, 33 (1974).
- <sup>41</sup> P. Tavan and K. Schulten, *Phys. Rev. B* **36**, 4337 (1987).
- <sup>42</sup> A. Köhler, D. A. dos Santos, D. Beljonne, Z. Shuai, J. L. Brédas, A. B. Holmes, A. Kraus, K. Müllen, and R. H. Friend, *Nature* **392**, 903 (1998).
- <sup>43</sup> M. Y. Lavrentiev, W. Barford, S. J. Martin, H. Daly, and R. J. Bursill, *Phys. Rev. B* **59**, 9987 (1999).
- <sup>44</sup> D. Beljonne, *Habilitation Thesis*, Université de Mons-Hainaut, Belgium (2001).
- <sup>45</sup> M. Chandross, S. Mazumdar, M. Liess, P. A. Lane, Z. V. Vardeny, M. Hamaguchi, and K. Yoshino, *Phys. Rev. B* **55**, 1486 (1997).
- <sup>46</sup> K. Ohno, *Theor. Chim. Acta* **2**, 219 (1964).
- <sup>47</sup> C. W. M. Castleton and W. Barford, *J. Chem. Phys.* **117**, 3570 (2002).
- <sup>48</sup> H. Ghosh, A. Shukla, and S. Mazumdar, *Phys. Rev. B* **62**, 12763 (2000).
- <sup>49</sup> D. Comoretto, G. Dellepiane, F. Marabelli, J. Cornil, D. dos Santos, J. Brédas, and D. Moses, *Phys. Rev. B* **62**, 10173 (2000).
- <sup>50</sup> E. K. Miller, D. Yoshida, C. Y. Yang, and A. J. Heeger, *Phys. Rev. B* **59**, 4661 (1999).
- <sup>51</sup> F. Guo, D. Guo, and S. Mazumdar, *Phys. Rev. B* **49**, 10102 (1994).
- <sup>52</sup> Z. G. Soos, S. Etemad, D. S. Galvao, and S. Ramasesha, *Chem. Phys. Lett.* **194**, 341 (1992).
- <sup>53</sup> M. Chandross and S. Mazumdar, *Phys. Rev. B* **55**, 1497 (1997).
- <sup>54</sup> D. L. Beveridge and H. H. Jaffe, *J. Am. Chem. Soc.* **87**, 5340 (1965).
- <sup>55</sup> E. E. Moore and D. Yaron, *J. Chem. Phys.* **109**, 6147 (1998).
- <sup>56</sup> S. Mazumdar, D. Guo, and S. N. Dixit, *J. Chem. Phys.* **96**, 6862 (1992).
- <sup>57</sup> M. G. Harrison, S. Moller, G. Weiser, G. Urbasch, R. F. Mahrt, H. Bässler, and U. Scherf, *Phys. Rev. B* **60**, 8650 (1999).
- <sup>58</sup> M. G. Harrison, G. Urbasch, R. F. Mahrt, H. Giessen, H. Bässler, and U. Scherf, *Chem. Phys. Lett.* **313**, 755 (1999).
- <sup>59</sup> M. Wohlgenannt, K. Tandon, S. Mazumdar, S. Ramasesha, and Z. V. Vardeny, *Nature (London)* **409**, 494 (2001).
- <sup>60</sup> K. Tandon, S. Ramasesha, and S. Mazumdar, *Phys. Rev. B* **xx**, xxxxxx (2003).

TABLE III: Relative weights of the dominant contributions to the excited states of different oligomers of PPP and PPV, computed with the screened Coulomb parameters (see text). Note that the  $d_3$  band does not occur in PPP

Oligmer	PA Feature	State	$d_1 \rightarrow d_1^*$	$d_1 \rightarrow d_2^*$	$d_1 \rightarrow d_3^*$	$(d_1 \rightarrow d_1^*)^2$	$(d_1 \rightarrow l^*)^2$
PPP4	I	$2A_g$	0.5546	0.0387	—	0.1121	—
	II	$3A_g$	0.0471	0.3396	—	0.2164	—
		$4A_g$	0.0779	0.1787	—	0.2997	0.0681
	III	$5A_g$	0.0385	0.2474	—	0.1037	0.0210
	IV	$8A_g$	—	0.3476	—	0.1566	0.0147
		$10A_g$	—	0.1848	—	0.0894	0.3289
PPP5	I	$2A_g$	0.6171	—	—	0.0903	—
	II	$4A_g$	0.1236	—	—	0.4688	0.0695
	III	$7A_g$	0.1309	—	—	0.4390	—
	IV	$9A_g$	—	0.2284	—	0.0543	0.2516
PPV3	I	$2A_g$	0.3872	—	—	0.2847	—
	II	$4A_g$	0.3042	0.0488	—	0.3313	0.0169
	III	$7A_g$	0.2732	0.1458	—	—	—
	IV	$10A_g$	—	0.0338	0.1746	0.0256	0.3193
PPV4	I	$2A_g$	0.5078	—	—	0.1884	—
	II	$3A_g$	0.1983	—	—	0.4680	—
	III	$4A_g$	0.4178	—	—	0.2483	—
		$5A_g$	0.0149	0.3366	—	0.2859	—
	IV	$9A_g$	0.0602	0.4555	—	0.0318	0.0398
	V	$12A_g$	—	0.1140	0.1460	0.02071	0.2284